A Complete Simulation of a Triple-GEM Detector

W. Bonivento, A. Cardini, G. Bencivenni, F. Murtas, and D. Pinci

***Abstract*—Since some years the gas electron multipliers (GEM)-based detectors have been proposed for many different applications, in particular, in high-energy physics and astrophysics experiments and medical imaging. Many experimental measurements and tests have been performed to investigate their characteristics and performances. To achieve a better understanding of the behavior of this kind of detector the computer simulation is a very important tool. In this paper, a complete and detailed simulation of a triple-GEM-based detector is described. A method has been developed to take into account all the processes from the ionization mechanism up to the signal formation and electronic response. The results obtained are compared with experimental data and a very good agreement is achieved.**

***Index Terms*—Gas electron multipliers (GEM), Garfield, simulation.**

I. Introduction

A GAS electron multiplier (GEM) [1] is a kapton foil, copper clad on each side, and perforated with a high surface density of holes. A potential difference of the order of 500 V applied between the two copper electrodes generates an electric field as high as 100 kV/cm into the holes, which may act as multiplication channels for the electrons created in a gas by an ionizing particle. The gain in the channel is of the order of $100 \div 200$, but only a part of the secondary electrons can leave the GEM foil and the effective gain results in about $20 \div 100$. Multiple GEM structures, allowing to reach a higher total gain ($10^4 \div 10^5$), are used to build detectors for charged particles and photons. In order to study the properties of a triple-GEM-based detector a full and detailed simulation has been performed. At first, single GEM characteristics have been investigated by using Maxwell [2] and Garfield [3]. The properties of a complete triple-GEM-based detector have been then derived by developing a Monte Carlo method. The readout electronics behavior has also been simulated by means of Spice [4] in order to compare the simulation results with experimental data.

II. Single GEM Simulation

A. The Model

The standard GEM (bi-conical holes with external diameter of 70 μm, internal diameter of 50 μm disposed with a pitch of 140 μm on staggered rows) operating in an $Ar/CO_2/CF_4$ (60/20/20) gas mixture has been simulated and studied.

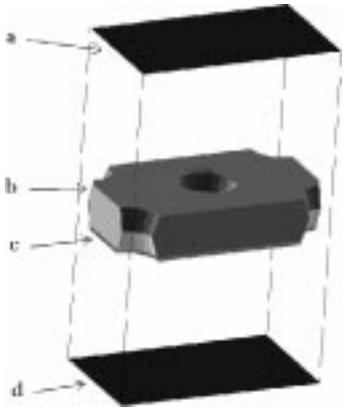

Fig. 1. GEM foil elementary "cell" layout used in Maxwell.

1) The Electric Field Configuration: A three-dimensional model, built within Maxwell, has been used to calculate the electric field map of GEM placed in an external electric field. This model (Fig. 1), based on a $400 \times 121 \times 70$ μm^3 elementary "cell," is made of a 50-μm-thick kapton clad on each side (b and c in the figure) with 5-μm-thick copper. The top and bottom of the box are equipotential planes, used to define the electric fields above and below the GEM foil. It is possible to reproduce different electrostatic configurations by changing the boundary conditions on the surfaces a, b, c, and d. Maxwell calculates, by means of the finite element method, the electric field maps. About 31 000 tetrahedrons have been used in this model, resulting in a system electrostatic energy error smaller than 0.04%.

It is possible to reproduce an entire GEM foil by replicating periodically this elementary "cell." In order to do that, only the tangential components of the electric field on the sides of the box have been taken into account.

2) The Gas Mixture: The gas mixture properties have been calculated using the following simulation tools.

- Magboltz [5] is used to compute the electrons drift velocity and the longitudinal and transverse diffusion coefficients.
- Heed [6] calculates the energy loss of a charged particle that crosses the gas volume through ionization and simulates the clusters production process.
- Imonte 4.5 [7] has been used to compute the Townsend and attachment coefficients.

The calculated electron drift velocity as a function of the electric field is shown in Fig. 2(a) compared with experimental data [8]. The distribution of the number of primary clusters produced by a minimum ionizing particle in a 3-mm gap, shown in Fig. 2(b), gives an average value of about 15 clusters.

Manuscript received November 26, 2001; revised April 17, 2002.

W. Bonivento is with the PPE Division, CERN, 1211 Geneva 23, Switzerland.

A. Cardini is with the INFN Sezione di Cagliari, 09042 Monserrato (Cagliari), Italy.

G. Bencivenni and F. Murtas are with the Laboratori Nazionali di Frascati, INFN, 00044 Frascati, Rome, Italy.

D. Pinci is with the INFN Sezione di Cagliari, 09042 Monserrato (Cagliari), Italy (e-mail: Davide.Pinci@ca.infn.it).

Digital Object Identifier 10.1109/TNS.2002.805170

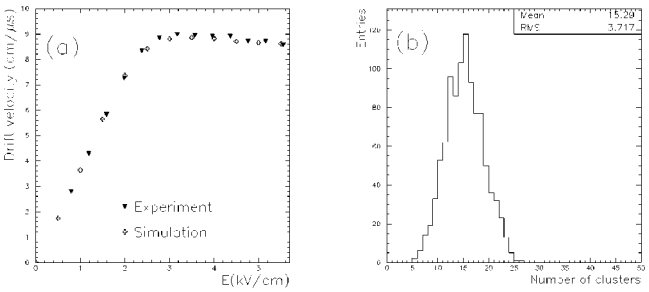

Fig. 2. $Ar/CO_2/CF_4$ (60/20/20) gas mixture properties. (a) Drift velocity obtained from experimental measurements [8] and from Garfield simulation. (b) Distribution of the number of primary clusters in a 3-mm gap obtained from Garfield simulation.

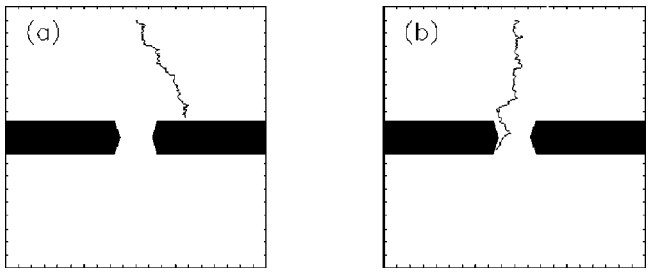

Fig. 3. Examples of simulated electron drift processes. (a) Electron hitting the upper GEM electrode. (b) Electron absorbed by the kapton walls into a GEM channel.

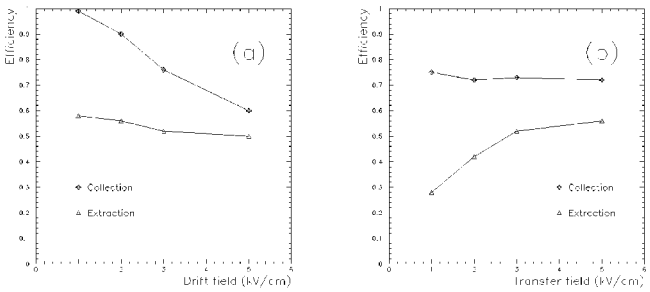

Fig. 4. Efficiencies dependence (a) on drift field and (b) on transfer field.

B. GEM Electron Transparency

Due to the diffusion effect and the electric field lines defocusing (i.e., some electric field lines above the GEM do not enter into the holes) electrons drifting in the gas can hit the upper GEM electrode [Fig. 3(a)]. Part of the electrons will also be captured by the kapton walls inside the channel because of the diffusion effect and by the lower GEM electrode because of the nonperfect electron extraction efficiency from the holes. [Fig. 3(b)]. Therefore, the GEM electron transparency T represents a very important parameter to be studied.

In order to evaluate the behavior of T as a function of the electric fields, simple studies have been performed. Electrons have been produced in a uniformly random position on a surface 150 μm above the GEM (where the equipotential surfaces are practically flat) and then a Monte Carlo drift process is generated. The ratio $(\text{number of } e^- \text{entering})/(\text{number of } e^- \text{generated})$ will be indicated as "collection efficiency" ϵ_{coll}, while the ratio $(\text{number of } e^- \text{extracted})/(\text{number of } e^- \text{ into the channel})$ will be indicated as "extraction efficiency" ϵ_{extr}. These parameters are related to T by

$$T = \epsilon_{\text{coll}} \cdot \epsilon_{\text{extr}} \tag{1}$$

The electric field above the GEM will be indicated as the "drift field" and the one below as the "transfer field."

- In Fig. 4(a), the dependence on the drift field is shown. The ϵ_{coll} decreases at high-drift field due to the defocusing effect, while ϵ_{extr} does not depend strongly on this parameter.
- In Fig. 4(b), the behavior for different transfer fields is shown. Due to a better electron extraction capability, ϵ_{extr} increases at high transfer fields.

It is important to note that the properties of one side of a GEM appear to depend only marginally on the electric field applied on the other side.

III. GEM GAIN

To study the single-GEM gain, electron avalanches into the channel are simulated with Garfield (Fig. 5). To perform a correct estimate of the gain, it is important to take into account the effect of diffusion. Thanks to diffusion, electrons can reach regions close to the hole sides where the higher electric field results in a higher multiplication.

The distribution of the number of secondary electrons leaving the GEM obtained by generating 1000 electrons on a surface 150 μm above a GEM with a U_{gem} of 450 V is shown in Fig. 6. The bin at zero represents the number of times no secondary electrons are extracted from the GEM. Its height is due to the nonperfect electron-transparency of the GEM (see Fig. 3).

For each single primary electron, large gain fluctuations have been found. The average number of secondary electrons produced will be indicated as "intrinsic gain" $\bar{G}_{\text{intr}}$, while the average number of secondary electron extracted will be indicated as the "effective gain" $\bar{G}_{\text{eff}}$ resulting in

$$\bar{G}_{\text{eff}} = \bar{G}_{\text{intr}} \cdot T \tag{2}$$

The dependences of $\bar{G}_{\text{intr}}$ and $\bar{G}_{\text{eff}}$ on the U_{gem} values are shown in Fig. 7(a) and (b).

IV. TRIPLE-GEM DETECTOR SIMULATION

Starting from the single GEM simulation the properties of a triple-GEM-based detector have been derived. The detector model used as a reference for the simulation and for the comparison is a triple-GEM prototype tested at the CERN PS T11 hadron beam line by the LHCb-muon group [11]. The geometric and electric configuration and the readout electronics parameters are summarized as follows:

- three standard GEM stacked one above the other, with $U_{\text{gem2}} = U_{\text{gem3}} = 390$ V;
- 3-mm drift gap with $E_d = 3$ kV/cm;
- 2-mm transfer gaps with $E_{t1} = E_{t2} = 4$ kV/cm;

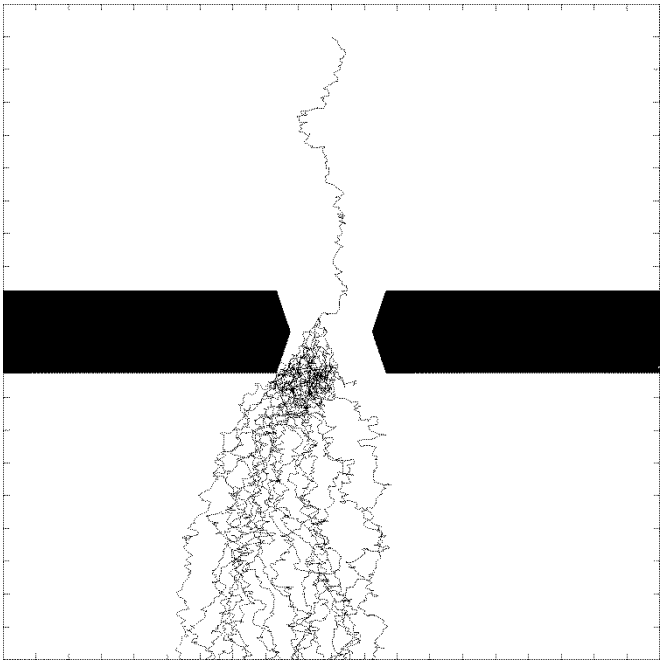

Fig. 5. Simulated avalanche developing in a GEM hole.

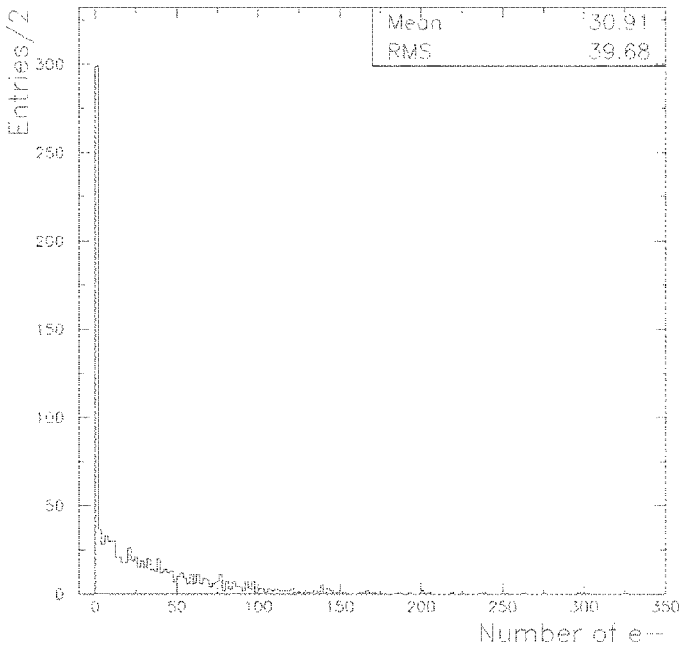

Fig. 6. Distribution of the number of secondary electrons extracted from the GEM foil.

- 1-mm induction gap with $E_i = 5$ kV/cm;
- discrete-components charge amplifier with a peaking time of 8 ns and a sensitivity of 10 mV/fC.

In order to evaluate the signal produced by a charged particle crossing the detector, the following physical processes have to be taken into account:

1) cluster creation and electron drift in the drift gap;
2) multiplication and electron transparency of each GEM;
3) charge transfer in the transfer gaps;
4) electron drift in the induction gap, signal formation, and electronics response.

A. Cluster Creation and Electron Drift

The number, position, and size of the clusters created by a charged particle crossing the detector have been calculated using Heed. Starting from the creation point, for each primary electron a drift process is simulated and the arrival time (t_d) on the first GEM is recorded.

The general expression for the probability distribution of the creation point distance from the first GEM x for the cluster j, when n is the average number produced is [9]

$$A_j^n(x) = \frac{x^{j-1}}{(j-1)!} n^j e^{-nx}. \tag{3}$$

It is possible to calculate (knowing the drift velocity v_d) the arrival time probability distribution, which results in

$$P_j(t_d) = v_d \cdot A_j^n(v_d t_d). \tag{4}$$

In particular, for the first cluster (the nearest to the first GEM)

$$P_1(t_d) = v_d \cdot n e^{-n v_d t_d}, \quad \sigma_1(t) = \frac{1}{n v_d} \tag{5}$$

where $\sigma_1(t)$ gives the intrinsic limit for the time resolution of a GEM-based detector when the first cluster is always detected. This limit depends only on the gas mixture properties and for the one used in the simulation $\sigma_1(t) = 2.2$ ns.

B. Detector Gain

The total gain is calculated for each primary electron. The total multiplication of any single electron of a cluster made by m primaries is simply given by the product of random-extracted values g_{eff} from the effective single GEM gain distribution. In this way, each cluster produced in the ionization gap becomes a cloud of n_{tot} electrons where

$$n_{\text{tot}} = \left(\Sigma_{i=1}^{m} g_{\text{eff1}}^i\right) \cdot g_{\text{eff2}} \cdot g_{\text{eff3}}. \tag{6}$$

In the first GEM, different gains are taken for each primary electron of a cluster. Due to the large number ($\simeq 30$) of secondary electrons leaving the first GEM the gains in the following GEMs have been approximated with the average values.

C. Charge Transfer

The transfer times (i.e., the times to cover the transfer gaps) t_{t1} and t_{t2} have also been calculated by the sum of random extracted values from the distributions of the electron drift times in the two transfer gaps. The electron cloud in the simulation arrives at the last gap at a time T_0 after the track crossing given by

$$T_0 = t_d + t_{t1} + t_{t2}. \tag{7}$$

The total arrival time spread can be calculated as

$$\sigma(T_0) = \sigma(t_d) \oplus \sigma(t_{t1}) \oplus \sigma(t_{t2}). \tag{8}$$

The simulation gives $\sigma(t_{t1}) = \sigma(t_{t2}) \simeq 0.5$ ns (which is due to the diffusion effect). Hence, the main contribution to the $\sigma(T_0)$ is expected to be given by $\sigma(t_d)$.

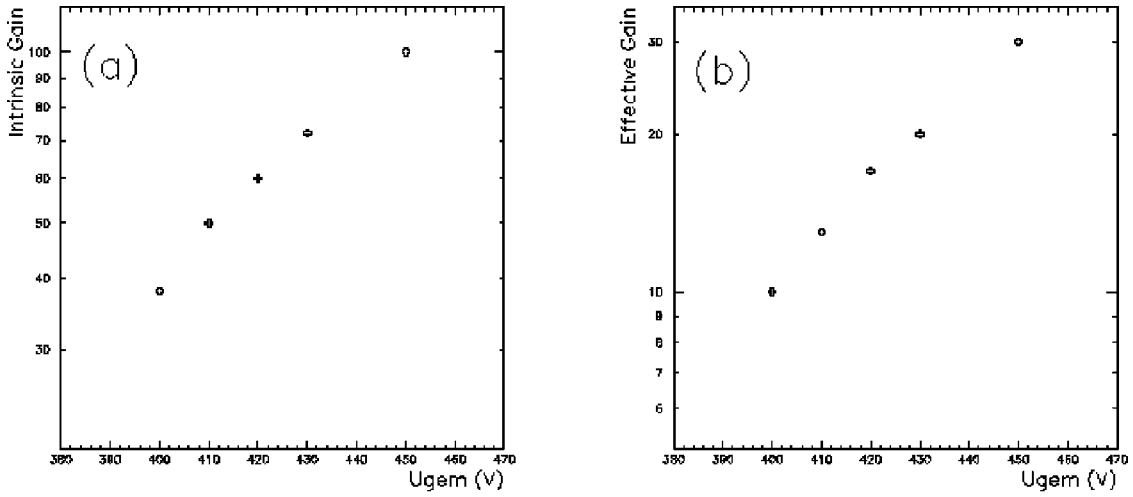

Fig. 7. (a) $\bar{G}_{\rm intr}$ and (b) $\bar{G}_{\rm eff}$ as a function of the GEM voltage supply.

D. Signal Formation

The signal is induced on the readout anode by the electron motion in the induction gap. The current flowing into an electrode k due to a moving charge q can be calculated using the Ramo's theorem [10]

$$I_k = \frac{-q\vec{v}(x) \times \vec{E}^k(x)}{V_k} \tag{9}$$

where the $\vec{E}^k(x)$ is the electric field created by raising the electrode k to the potential V_k (all other electrodes being at 0 V). In particular, if $V_k = 1$ V, the resulting electric field is called "weighting field" ($\vec{E}^k_w$) and the Ramo's theorem becomes

$$I_k = -q\vec{v}(x) \times \vec{E}^k_w(x). \tag{10}$$

In this detector, $\vec{E}^k_w(x)$ is almost constant and then a single electron induces a constant current of -14 pA for about 11 ns.

E. Electronics Simulation

The transfer function of the readout electronics has been evaluated with Spice. The total signal due to a minimum ionizing particle has been calculated by convoluting the signals of all electron clouds, which start at different T_0 (Fig. 8). It is possible to see the following:

1) signal rise due to the arrival of the first electron cloud in the last gap;
2) flat part of the signal, visible between $t = 45$ ns and $t = 55$ ns due to the constant $\vec{E}_w$;
3) duration time is about 30 ns, which corresponds to the maximum drift time in the ionization gap.

F. The Noise

A very important role in the detector performances is played by the electronics noise which decreases the time resolution. From the electronics rise time t_r ($\simeq$ 6 ns) the upper 3-dB frequency f_h could be calculated from the relationship [12]

$$f_h \cdot t_r \simeq 0.35 \tag{11}$$

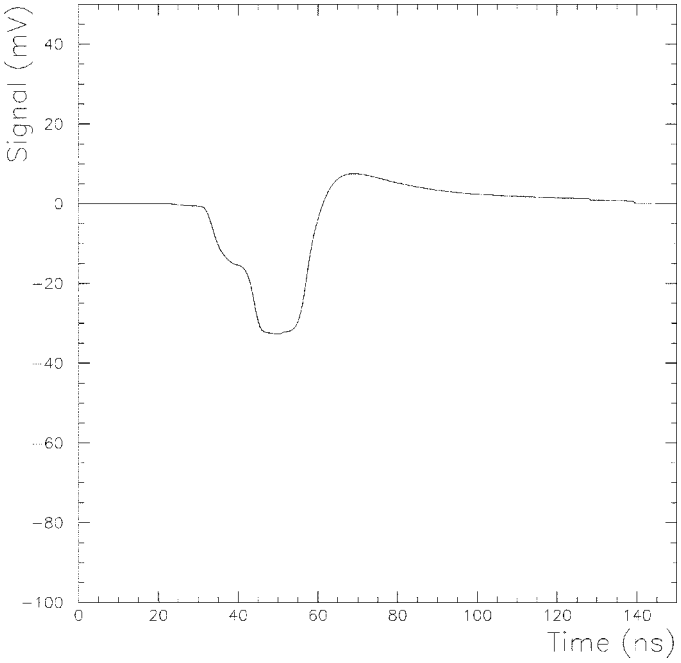

Fig. 8. Signal due to a track from the simulation.

which gives $f_h = 60$ MHz. The noise frequency distribution has been approximated to be flat up to $3 \cdot f_h$ and zero after. The noise amplitude has been chosen to be Gaussian distributed with mean 0 and root mean square (RMS) tuned to reproduce the noise seen by the charge measuring device (ADC) pedestal width ($\simeq$ 30 counts) measured at the test beam, where an ADC with 50 fC/count sensitivity and a 200 ns gate was used.

V. Simulation Results

Using the method and tools described in previous sections, the detector main characteristics have been simulated and studied in details.

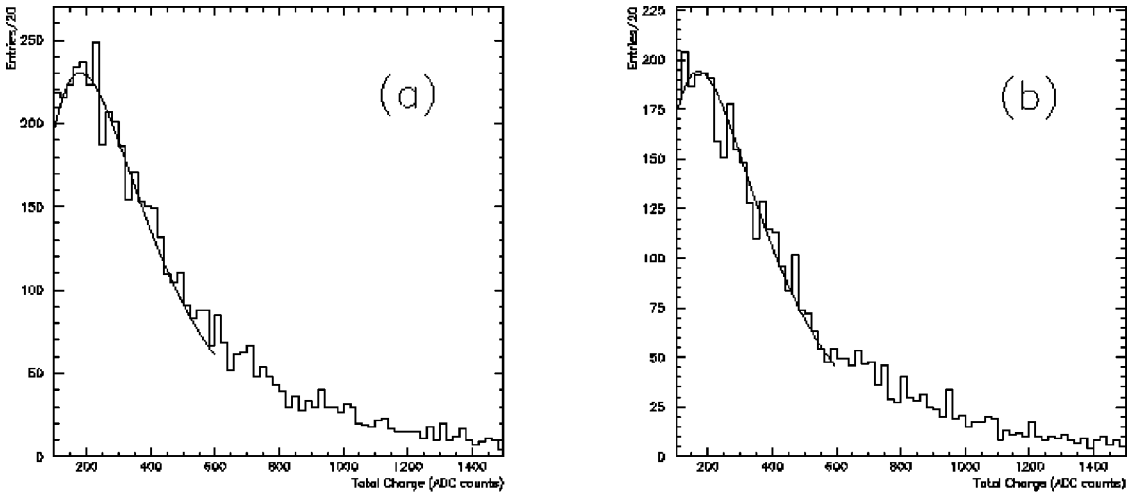

Fig. 9. (a) Experimental and (b) simulated detector total charge spectra.

A. Detector Total Gain

A first study has been performed on the detector total gain (i.e., the 3-GEM gain and the electronics gain). The total charge spectra have been calculated as a function of U_{gem1}. The simulated total charge has been found to be lower than the experimental one as it was found also by other authors [13]. In the whole range $U_{\mathrm{gem1}} = 400\ \mathrm{V} \rightarrow 450\ \mathrm{V}$, a factor 3 has been used to adjust the total gain of the detector coming from the simulation. This discrepancy might be due to the fact that the Townsend coefficient calculated with Imonte and used in the simulation may not reproduce exactly the real one. Studies to clarify this discrepancy are under way. Taken into account this overall re-calibration factor a very good agreement between simulation and experimental data has been obtained. The charge spectra obtained with $U_{\mathrm{gem1}} = 420\ \mathrm{V}$ are shown in Fig. 9. In Fig. 10 the peak positions of the total charge spectra obtained with the simulation are compared with the experimental ones.

B. Detector Efficiency and Time Resolution

The total efficiency and the efficiency in a 25-ns time-window have been calculated. These parameters are very important in order to understand if GEM-based detectors could be used for triggering at the future Large Hadron Collider (LHC) under construction at CERN event rates.

To obtain the correct values for the efficiency in a 25-ns time-window the so-called bi-GEM effect has to be included. This effect is due to the possibility that the ionization produced in the first transfer gap could be amplified by the second and third GEM enough to be discriminated, resulting in an out-of-time (i.e., early) hit, which worsens the time resolution. The experimental fraction of events due to bi-GEM effect is 1.3% while from the simulation a value of 1.4% has been found. This value has been subtracted from the 25-ns time-window efficiency. In Fig. 11 are shown the behaviors of the (a) experimental and simulated total and (b) in a 25-ns time-window efficiencies as a function of U_{gem1} with a discriminator threshold of 12 mV. The

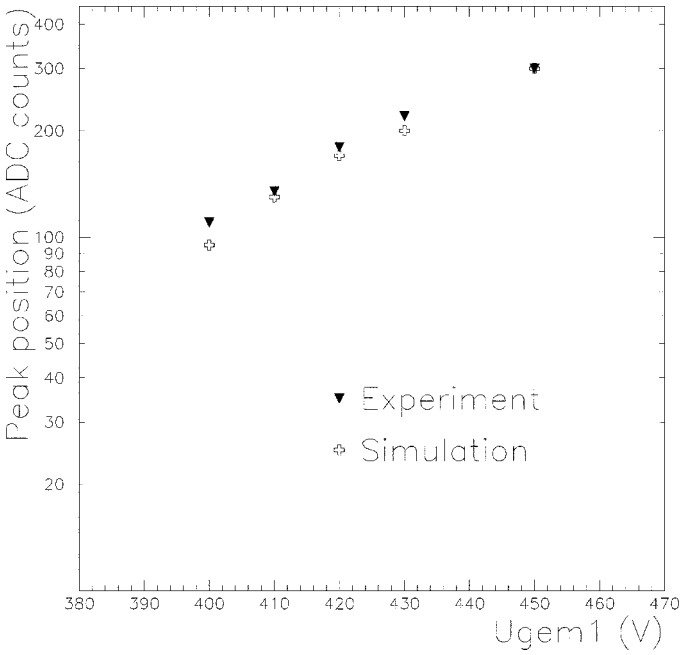

Fig. 10. Position of the Landau distribution peaks from experimental data and simulation.

detector total efficiency and the time resolution increase by increasing U_{gem1}. The latter shows a stronger dependence on this parameter which could be explained by an improvement of the single electron detection capability of the detector for an high total gain. This results in a big reduction of the time distribution tail due to events in which the first cluster is lost and, hence, in a better time resolution.

VI. Conclusion

A big effort has been necessary to obtain a correct model of triple GEM detectors. The results obtained after a recalibration of the total gain of a factor 3 show a very good agreement with the experimental data. The charge spread has not been taken into account. This could indicate that it does not play any crucial role

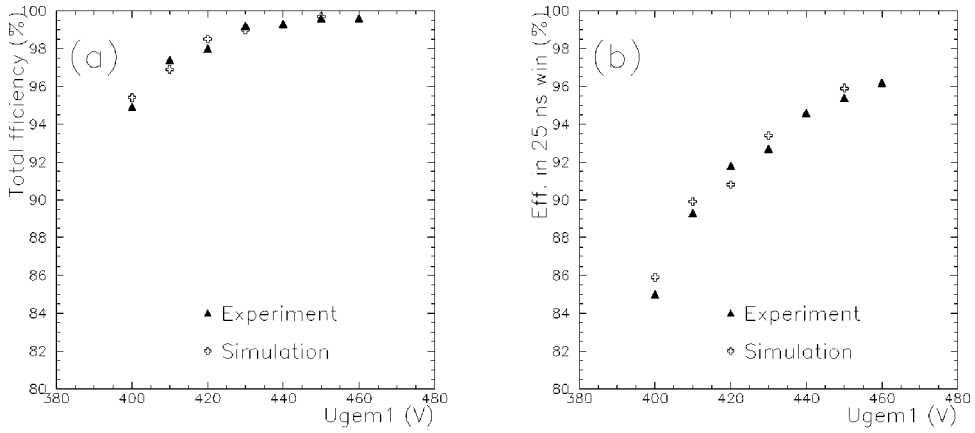

Fig. 11. Experimental and simulated (a) total and (b) in a 25-ns window-detector efficiency as function of U_{gem1}.

in the detector performances studied in this work. The method developed here can be used to achieve a better understanding of the behavior of the GEM and to optimize the detector characteristics (geometry, gas mixture, electric fields configuration. . .) in order to improve the real detector performances.

REFERENCES

[1] F. Sauli, "GEM: A new concept for electron amplification in gas detectors," *Nucl. Instrum. Methods*, vol. A 386, pp. 531–534, 1997.

[2] *Maxwell 3D Field Simulator User's Reference*, Ansoft Corp., Pittsburgh, PA, 1999.

[3] R. Veenhof, "Garfield, recent developments," *Nucl. Instrum. Methods*, vol. A 419, pp. 726–730, 1998.

[4] L. W. Nagel and D. O. Pederson, "Spice (simulation program with integrated circuit emphasis)," presented at the ERL-M382 16th Midwest Symp. Circuit Theory, Waterloo, ON, Canada, Apr. 12, 1973.

[5] S. Biagi. (2000) Magboltz—A program to solve the Boltzmann transport equations for electrons in gas mixtures. CERN, Geneva, Switzerland. [Online]. Available: http://consult.cern.ch/writeup/magboltz

[6] I. Smirmov. (1997) HEED—A program to compute energy loss of fast particle in a gas. CERN, Geneva, Switzerland. [Online]. Available: http://consult.cern.ch/writeup/heed

[7] S. Biagi, "Monte Carlo simulation of electron drift and diffusion in counting gases under the influence of electric and magnetic fields," *Nucl. Instrum. Methods*, vol. A 421, pp. 234–240, 1999.

[8] U. Becker, R. Dinner, E. Fortunato, J. Kirchner, K. Rosera, and Y. Uchida, "Consistent measurements comparing the drift features of noble gas mixtures," *Nucl. Instrum. Methods*, vol. A 421, pp. 54–59, 1999.

[9] F. Sauli, "Principles of operation of multiwire proportional and drift chamber," CERN, Geneva, Switzerland, Rep. 77-09, 1977.

[10] S. Ramo, "Currents induced by electron motion," in *Proc. IRE 27*, 1939, pp. 584–585.

[11] G. Bencivenni, G. Felici, F. Murtas, P. Valente, W. Bonivento, A. Cardini, A. Lai, D. Pinci, and B. Saitta, "A triple GEM detector with pad readout for inner region of the first LHCb muon station," CERN, Geneva, Switzerland, LHCb 2001-051, 2001.

[12] P. W. Nicholson, *Nuclear Electronics*. New York: Wiley, 1974.

[13] A. Sharma, "3D simulation of charge transfer in a gas electron multiplier (GEM) and comparison to experiment," *Nucl. Instrum. Methods*, vol. A 454, pp. 267–271, 2000.